Targeting of HER2-Expressing Tumors with a Site-Specifically ^{99m}Tc-Labeled Recombinant Affibody Molecule, $Z_{HER2:2395}$, with C-Terminally Engineered Cysteine

Sara Ahlgren[1], Helena Wållberg[2], Thuy A. Tran[3], Charles Widström[4], Magnus Hjertman[2], Lars Abrahmsén[2], Dietmar Berndorff[5], Ludger M. Dinkelborg[5], John E. Cyr[5], Joachim Feldwisch[2,3], Anna Orlova[2,3], and Vladimir Tolmachev[1–3]

[1]Division of Nuclear Medicine, Department of Medical Sciences, Uppsala University, Uppsala, Sweden; [2]Affibody AB, Bromma, Sweden; [3]Rudbeck Laboratory, Division of Biomedical Radiation Sciences, Department of Radiology, Oncology, and Clinical Immunology, Uppsala University, Uppsala, Sweden; [4]Hospital Physics, Department of Oncology, Uppsala University Hospital, Uppsala, Sweden; and [5]Global Drug Discovery, Bayer Schering Pharma AG, Berlin, Germany

The detection of human epidermal growth factor receptor type 2 (HER2) expression in malignant tumors provides important information influencing patient management. Radionuclide in vivo imaging of HER2 may permit the detection of HER2 in both primary tumors and metastases by a single noninvasive procedure. Small (7 kDa) high-affinity anti-HER2 Affibody molecules may be suitable tracers for SPECT visualization of HER2-expressing tumors. The use of generator-produced ^{99m}Tc as a label would facilitate the prompt translation of anti-HER2 Affibody molecules into use in clinics. **Methods:** A C-terminal cysteine was introduced into the Affibody molecule $Z_{HER2:342}$ to enable site-specific labeling with ^{99m}Tc. Two recombinant variants, His_6-$Z_{HER2:342}$-Cys (dissociation constant [K_D], 29 pM) and $Z_{HER2:2395}$-Cys, lacking a His tag (K_D, 27 pM), were labeled with ^{99m}Tc in yields exceeding 90%. The binding specificity and the cellular processing of Affibody molecules were studied in vitro. Biodistribution and γ-camera imaging studies were performed in mice bearing HER2-expressing xenografts. **Results:** ^{99m}Tc-His_6-$Z_{HER2:342}$-Cys was capable of targeting HER2-expressing SKOV-3 xenografts in SCID mice, but the liver radioactivity uptake was high. A series of comparative biodistribution experiments indicated that the presence of the His tag caused elevated accumulation in the liver. ^{99m}Tc-$Z_{HER2:2395}$-Cys, not containing a His tag, showed low uptake in the liver and high and specific uptake in HER2-expressing xenografts. Four hours after injection, the radioactivity uptake values (percentage of injected activity per gram of tissue [%IA/g]) were 6.9 ± 2.5 (mean ± SD) %IA/g in LS174T xenografts (moderate level of HER2 expression) and 15 ± 3 %IA/g in SKOV-3 xenografts (high level of HER2 expression). The corresponding tumor-to-blood ratios were 88 ± 24 and 121 ± 24, respectively. Both LS174T and SKOV-3 xenografts were clearly visualized with a clinical γ-camera 1 h after injection of ^{99m}Tc-$Z_{HER2:2395}$-Cys. **Conclusion:** The Affibody molecule ^{99m}Tc-$Z_{HER2:2395}$-Cys is a promising tracer for SPECT visualization of HER2-expressing tumors.

Received Aug. 12, 2008; revision accepted Feb. 5, 2009.
For correspondence or reprints contact: Vladimir Tolmachev, Rudbeck Laboratory, Division of Biomedical Radiation Sciences, Uppsala University, SE-751 85 Uppsala, Sweden.
E-mail: Vladimir.Tolmachev@bms.uu.se

Key Words: Affibody molecule; technetium; imaging; HER2; C-terminal cysteine

J Nucl Med 2009; 50:781–789
DOI: 10.2967/jnumed.108.056929

Human epidermal growth factor receptor type 2 (HER2) is a transmembrane protein belonging to the receptor tyrosine kinase superfamily (*1*). HER2 signaling is associated with increased proliferation and decreased apoptotic capacity (*2*). Overexpression of HER2 is found in a variety of cancers, for example breast, ovary, colorectal, and urothelial carcinomas, and is associated with more aggressive disease and a poor prognosis (*1*). This receptor is the target for therapy with the monoclonal antibody trastuzumab (Herceptin; Roche Pharma AG), which interrupts HER2 signaling and prolongs the survival of patients with HER2-expressing breast cancer (*3,4*). HER2 is, however, overexpressed in only 25%−30% of breast carcinomas. Therefore, the detection of HER2 expression is necessary to identify patients who would benefit from trastuzumab therapy. Both the American Society of Clinical Oncology and the European Group on Tumor Markers have recommended that HER2/c-erbB-2 overexpression should be evaluated for every primary breast cancer (*5,6*).

Most commonly, HER2 status is determined by immunohistochemical or fluorescent in situ hybridization analysis of biopsy material. Unfortunately, the results of such tests may be adversely affected by tumor sampling errors, discordance in HER2 expression in primary tumors and metastases, and inexperience of laboratories performing analyses (*7*). The use of radionuclide molecular imaging of HER2 expression may help to avoid these problems associated with biopsies. Moreover, radionuclide imaging may also allow determination of the HER2 expression status in

lesions not amenable to biopsy, for example, bone metastases.

Clinical studies on the radionuclide imaging of HER2 were initially performed with ^{111}In-labeled trastuzumab (*8,9*). However, the detection sensitivity was not optimal. Only 45% of the lesions already detected by routine imaging techniques were detected by the radionuclide scan (*9*). Low sensitivity is a general problem when full-size IgG antibodies are used as targeting agents because their long residence time in blood causes high radioactivity background, leading to reduced imaging contrast. An analysis of preclinical data showed that smaller tracers provide better imaging contrast and therefore better sensitivity than intact antibodies (*10*).

The problem of size reduction for a HER2-targeting agent could be solved with Affibody molecules (*11*). Affibody molecules originate from the 58-amino-acid (7 kDa) cysteine-free scaffold of the staphylococcal protein A–derived Z domain. The scaffold has been subjected to the randomization of 13 surface-exposed residues to generate a library from which high-affinity binders can be selected by phage display. The selection of the Affibody molecule $Z_{HER2:342}$, which binds to the extracellular domain of HER2 with an affinity of 22 pM, was described earlier (*12*). High-contrast imaging of HER2-expressing xenografts with indirectly radioiodinated $Z_{HER2:342}$ was demonstrated (*12*). The potential of recombinant Affibody molecules for imaging was confirmed in preclinical studies with radioisotopes of bromine (*13*) and indium in combination with various chelators (*14–16*).

The spontaneously folding structure of Affibody molecules is amenable to complete peptide synthesis of a well-defined product and site-specific incorporation of various functional groups. Synthetic Affibody molecule $Z_{HER2:342}$ with DOTA incorporated at the N-terminus has been prepared, labeled with ^{111}In, and characterized in vivo (*17*). The imaging of HER2-expressing metastases with ^{111}In- and ^{68}Ga-labeled DOTA-$Z_{HER2:342}$ has been demonstrated in clinical case studies (*18*).

Generator-produced ^{99m}Tc (half-life = 6 h) is an attractive radionuclide for molecular imaging applications because of its photon energy (which is nearly ideal for SPECT), low cost, excellent availability, and low dose burden for the patient. Earlier, mercaptoacetyl-containing synthetic Affibody molecules were labeled with ^{99m}Tc and demonstrated high-contrast imaging of HER2-expressing xenografts (*19–21*).

Mercaptoacetyl is added during chemical peptide synthesis; this process may be applicable only to smaller peptides and monomer Affibody molecules. Therefore, several approaches have been pursued to obtain site-specific labeling of recombinant proteins. We previously reported on the ^{99m}Tc labeling of His tag–containing anti-HER2 Affibody dimers with technetium(I) tricarbonyl chemistry (*22*). Unfortunately, this kind of labeling resulted in high radioactivity uptake in the liver. The absence of cysteine residues in the Affibody scaffold enables the creation of a unique reactive site through the incorporation of a single cysteine. The Cys thiol group, along with 3 amides in the peptide backbone, creates a site-specific N_3S chelator for labeling with ^{99m}Tc, resulting in a controlled, homogeneous product. This approach has been applied for the labeling of single-chain Fv fragments (*23–25*). We previously evaluated the labeling of Affibody molecules with CGG and CGGG sequences incorporated at the N terminus of Affibody molecule $Z_{HER2:342}$ (*26*). The ^{99m}Tc-CGG-$Z_{HER2:342}$ conjugate was capable of specifically targeting HER2-expressing xenografts in mice and provided a tumor-to-blood ratio of 9.2 (6 h after injection). However, radioactivity uptake in the stomach and salivary glands was higher than that obtained with mercaptoacetyl-containing conjugates, indicating the release of free pertechnetate during catabolism of the conjugate in vivo. Placement of the cysteine residue in a C-terminal position allows for a more stable "GGC"-type chelator, as previously demonstrated for scFv fragments and for technetium-labeled peptide radiopharmaceuticals (*27*). In a GGC–technetium complex, the N_3S ligand set forms a stable chelate with three 5-member rings during complexation with the technetium; however, when the cysteine is located at the N-terminus (CGG), metal complexation through the cysteine yields a 6-member ring in the chelate, which is known to yield a less stable technetium(V) complex (*28*).

The goal of the study was to evaluate whether the introduction of a single cysteine at the C-terminus of recombinant Affibody molecules would provide stable labeling with ^{99m}Tc. An initial characterization was performed with His tag–containing ^{99m}Tc-His_6-$Z_{HER2:342}$-Cys (hereafter referred to as ^{99m}Tc-H_6-$Z_{HER2:342}$-C) because a His tag facilitates the purification of recombinant proteins. The biodistribution of ^{99m}Tc-H_6-$Z_{HER2:342}$-C demonstrated high radioactivity uptake in the liver. Further in vivo studies demonstrated that this elevated liver uptake was associated with the presence of the His tag. An Affibody molecule lacking the His tag, $Z_{HER2:2395}$-Cys (hereafter referred to as Z_{2395}-C), showed low uptake in the liver and good targeting properties when radiolabeled with ^{99m}Tc. γ-camera imaging confirmed that ^{99m}Tc-Z_{2395}-C was capable of specific imaging of HER2-expressing xenografts.

MATERIALS AND METHODS

Materials

^{99m}Tc was obtained as pertechnetate by elution in an Ultra-TechneKow generator (Tyco) with sterile 0.9% sodium chloride (Mallinckrodt Medical BV). An automated γ-counter with a ~7.6-cm (3-in) NaI(Tl) detector (1480 WIZARD; Wallac Oy) was used to detect radioactivity. A Cyclone storage phosphor system and OptiQuant image analysis software (both from Perkin-Elmer) were used to measure the radioactivity on instant thin-layer chromatography silica gel–impregnated (ITLC SG) strips. Affibody molecules H_6-$Z_{HER2:342}$-C and Z_{2395}-C were produced and purified as described by Ahlgren et al. (*29*). These two proteins differ only

in the N-terminal sequence (**GSSHHHHHHLQVD**NKFNK for H_6-$Z_{HER2:342}$-C and **AE**NKFNK for Z_{2395}-C [differences are shown in bold type]).

Labeling Chemistry and In Vitro Characterization

Cysteine-containing HER2-binding Affibody molecules were site-specifically labeled with ^{99m}Tc by use of freeze-dried labeling kits each containing 5 mg of sodium α-D-glucoheptonate dihydrate, 100 μg of edetate disodium (EDTA), and 50 μg of tin(II) chloride dihydrate ($SnCl_2 \cdot 2H_2O$) at pH 7.4. The freeze-dried kits were stored at −20°C.

For radiolabeling of ^{99m}Tc-H_6-$Z_{HER2:342}$-C, a ^{99m}Tc-pertechnetate generator eluate (370 MBq; 350 μL), Affibody molecule H_6-$Z_{HER2:342}$-C dissolved in phosphate-buffered saline (PBS; 200 μg; 91 μL), and 560 μL of saline were added to a freeze-dried kit, and the contents of the vial were swirled. The vial was incubated for 10 min at 100°C and cooled for 15 min at room temperature. The radiochemical purity of ^{99m}Tc-H_6-$Z_{HER2:342}$-C was determined by reverse-phase high-pressure liquid chromatography with a water–acetonitrile gradient containing trifluoroacetic acid (supplemental Fig. 1) (supplemental materials are available online only at http://jnm.snmjournals.org). No further purification was needed.

For ^{99m}Tc-Z_{2395}-C, the labeling was reoptimized. Radiolabeling was performed by adding the contents of one freeze-dried kit, dissolved in PBS, to 100 μg of Affibody molecule Z_{2395}-C to a total volume of 100 μL. To the reaction solution, 100 μL of a ^{99m}Tc-pertechnetate generator eluate (typically, 50 MBq) was added under argon gas, and the solution was incubated at 90°C for 40 min and cooled at room temperature for 15 min. Thereafter, 1 μL samples were taken for analysis of the labeling yield by ITLC SG with PBS as the mobile phase and for analysis of reduced hydrolyzed technetium colloid levels by ITLC SG with pyridine:acetic acid:water (5:3:1.5) as the mobile phase. No further purification was needed. For in vitro and in vivo experiments, the labeling solution was diluted with PBS.

To test the labeling stability in vitro, two 5 μL samples of ^{99m}Tc-Z_{2395}-C were mixed with 100 μL of mouse plasma. After incubation at 37°C for 2 h, 20 μL of each sample was electrophoresed on a sodium dodecyl sulfate–polyacrylamide gel along with a sample of free $^{99m}TcO_4^-$ diluted in PBS.

The in vitro binding specificity of ^{99m}Tc-Z_{2395}-C was verified in HER2-expressing SKOV-3 ovarian carcinoma cells by receptor presaturation with unlabeled Affibody molecules as described by Ahlgren et al. (*29*). Antigen-binding capacity after radiolabeling was studied as described by Tran et al. (*26*). Cellular retention and internalization of radioactivity were evaluated as described by Ahlgren et al. (*29*).

Animal Studies

The animal experiments were planned and performed in accordance with national legislation on the protection of laboratory animals. The animal study plans were approved by the local ethics committee for animal research. Biodistribution studies with non–tumor-bearing mice were performed with female immunocompetent NMRI mice.

In experiments with tumor-bearing mice, female outbred BALB/c *nu/nu* or SCID mice were used. Xenografts of HER2-expressing LS174T colon adenocarcinoma cells and SKOV-3 cells were subcutaneously implanted in the right hind leg. For xenografts in BALB/c *nu/nu* mice, 10^6 LS174T cells or 10^7 SKOV-3 cells were used, whereas in SCID mice, 5×10^6 SKOV-3 cells were used. As negative controls for use in the imaging experiment, mice were given xenografts of 10^7 non–HER2-expressing A431 cells. At the time of the biodistribution experiment, the average (mean ± SD) tumor sizes were 0.3 ± 0.15 g for LS174T xenografts in BALB/c *nu/nu* mice, 0.4 ± 0.1 g for SKOV-3 xenografts in BALB/c *nu/nu* mice, and 1.0 ± 0.5 g for SKOV-3 xenografts in SCID mice.

For biodistribution studies with SKOV-3 xenograft–bearing SCID mice, animals were randomized into groups of 3 and injected intravenously with 60 ng of ^{99m}Tc-H_6-$Z_{HER2:342}$-C conjugate (94 kBq) in 100 μL of PBS. For studies with xenograft-bearing BALB/c *nu/nu* mice, animals were randomized into groups of 4 and injected intravenously with 1 μg of conjugate (50 kBq) in 100 μL of PBS. At predesignated time points, the mice were euthanized by anesthesia overdosing. Blood was collected by heart puncture. Organ samples were collected in preweighed plastic vials. All tissue uptake values were calculated as the percentage of injected activity (%IA) per gram of tissue (%IA/g), except for the thyroid, gastrointestinal tract, and carcass, where the tissue uptake values were calculated as the %IA per whole sample. The radioactivity in the gastrointestinal tract and its contents was used as a measure of hepatobiliary excretion.

The biodistributions of ^{99m}Tc-Z_{2395}-C and ^{99m}Tc-H_6-$Z_{HER2:342}$-C in NMRI mice were compared at 4 h after injection to verify that the elevated uptake in the liver was attributable to the His tag.

The biodistribution of ^{99m}Tc-Z_{2395}-C in BALB/c mice bearing LS174T xenografts was measured at 0.5, 1, 4, and 6 h after injection, and in BALB/c *nu/nu* mice bearing SKOV-3 xenografts at 4 h after injection (Table 3). To verify the specificity of HER2 targeting, HER2 was presaturated in one group of mice bearing LS174T xenografts and in another group of mice bearing SKOV-3 xenografts by subcutaneous injection with 600 μg of unlabeled His_6-$Z_{HER2:342}$ 45 min before injection of ^{99m}Tc-Z_{2395}-C. The animals were euthanized 4 h after injection, and uptake in tumors was measured.

For γ-camera imaging, two groups of LS174T xenograft–bearing mice were injected with 1.5 MBq of ^{99m}Tc-Z_{2395}-C (amount of protein, 3 μg). In a blocking experiment, one animal from each group was preinjected with unlabeled Affibody molecules as described earlier. One group of animals was euthanized 1 h after injection, and the other group was euthanized 4 h after injection. For imaging of SKOV-3 xenograft–bearing mice, 4 animals were injected with 1.5 MBq of ^{99m}Tc-Z_{2395}-C (amount of protein, 3 μg). Two of them were euthanized 1 h after injection, and the other two were euthanized 4 h after injection. As a negative control, two animals bearing non–HER2-expressing A431 xenografts were injected with the same amount of ^{99m}Tc-Z_{2395}-C as the SKOV-3 xenograft–bearing mice and euthanized 4 h after injection. All animals were euthanized by overdose with ketamine hydrochloride (Ketalar; Pfizer) and xylazine hydrochloride (Rompun; Bayer). After euthanasia, the urinary bladders were dissected. Imaging was performed at the Department of Nuclear Medicine at Uppsala University Hospital with an e.Cam γ-camera (Siemens Medical Systems, Inc.) equipped with a low-energy, high-resolution collimator. Acquisition of static images was performed with a 256 × 256 matrix and a zoom factor of 3.2. The energy window settings were 140 keV and 15%. The images were evaluated with Osiris 4.19 software (Digital Imaging Group, University Hospital of Geneva).

RESULTS

Analysis of Peptides

Data concerning the characterization of recombinant Affibody molecules were reported by Ahlgren et al. (*29*). All purified proteins demonstrated a single peak on liquid chromatography–mass spectrometry with a mass coinciding with the theoretically calculated value ± 1.5 Da, which is within the accuracy of the instrument. The introduction of a cysteine at the C terminus did not have an effect on the binding to HER2 because the apparent dissociation constants (K_D) of 29 pM for H_6-$Z_{HER2:342}$-C and 27 pM for Z_{2395}-C did not deviate from the K_D for parental Affibody molecule $Z_{HER2:342}$ (22 pM) and were within the accuracy of the measurement method.

Labeling Chemistry and In Vitro Characterization

The radiochemical purity determined by reverse-phase high-pressure liquid chromatography for ^{99m}Tc-H_6-$Z_{HER2:342}$-C was 93%. For ^{99m}Tc-Z_{2395}-C samples, labeling yields determined by ITLC were greater than 97%, and the levels of reduced hydrolyzed technetium colloids were less than 1%. A specific radioactivity of 3.5 GBq/μmol was achieved for ^{99m}Tc-Z_{2395}-C. Phosphorimaging analysis of the radioactivity distribution on a sodium dodecyl sulfate–polyacrylamide gel showed that after incubation at 37°C for 2 h in mouse plasma, 96% ± 0.2% of the radioactivity was associated with ^{99m}Tc-Z_{2395}-C and the rest of the radioactivity matched free $^{99m}TcO_4^-$. For biologic experiments, all ^{99m}Tc conjugates were used without additional purification.

In the in vitro specificity analysis, presaturation of HER2 in SKOV-3 cells with nonlabeled Affibody molecules reduced the cell-bound radioactivity from 30.3% ± 0.9% to 0.9% ± 0.1% ($P < 10^{-6}$) after 1 h of incubation at 37°C (Fig. 1A). This finding indicated that the binding of ^{99m}Tc-Z_{2395}-C to HER2-expressing cells was specific. The antigen-binding capacity after radiolabeling was 86% ± 1.6% when tested with SKOV-3 cells. The cellular retention and internalization analyses of ^{99m}Tc-Z_{2395}-C indicated that the conjugate was efficiently retained by HER2-expressing cells (Fig. 1B). The cellular retention of the total radioactivity was good, with 68% ± 1% being cell associated after 24 h of incubation at 37°C. The internalization of ^{99m}Tc-Z_{2395}-C was relatively slow, with less than 11% internalized radioactivity after 24 h. Most of the radioconjugate was released within the first 0.5 h, with a slow increase of released radioactivity up to 8 h. Thereafter, the levels were almost stable up to 24 h.

Animal Studies

The biodistribution data for ^{99m}Tc-H_6-$Z_{HER2:342}$-C in SCID mice are shown in Table 1. The conjugate showed rapid tumor targeting and rapid clearance from a majority of nontarget organs. Kidney uptake was high because of renal excretion and reabsorption; this pattern is typical for radiometal-labeled Affibody molecules. Liver uptake was also high (about 20 %IA/g); this finding is unusual for $Z_{HER2:342}$ conjugates. To examine whether the atypical liver uptake was attributable to the physiologic features of the mouse strain used (SCID), the biodistribution of a different $Z_{HER2:342}$-based tracer, ^{111}In-tetraazacyclododecanetetraacetic acid (DOTA)-$Z_{HER2:342}$, was investigated in SCID mice bearing SKOV-3 xenografts (Supplemental Table 1). The biodistribution data for ^{111}In-DOTA-$Z_{HER2:342}$ in SCID mice showed a high level of agreement with previously published data on biodistribution in BALB/c *nu/nu* mice (*17*).

A comparison of the biodistributions of the His tag–containing conjugate, ^{99m}Tc-H_6-$Z_{HER2:342}$-C, and a corresponding conjugate lacking the His tag, ^{99m}Tc-Z_{2395}-C, is shown in Figure 2. The general biodistributions for both conjugates were similar, except that the His tag–containing conjugate showed elevated (nearly 5-fold) uptake of radioactivity in the liver 4 h after injection ($P < 10^{-4}$). This finding is a strong indication that the His tag inherently increases liver uptake and, thus, that His tag–containing conjugates are less suitable for future imaging applications. Therefore, only ^{99m}Tc-Z_{2395}-C was evaluated further.

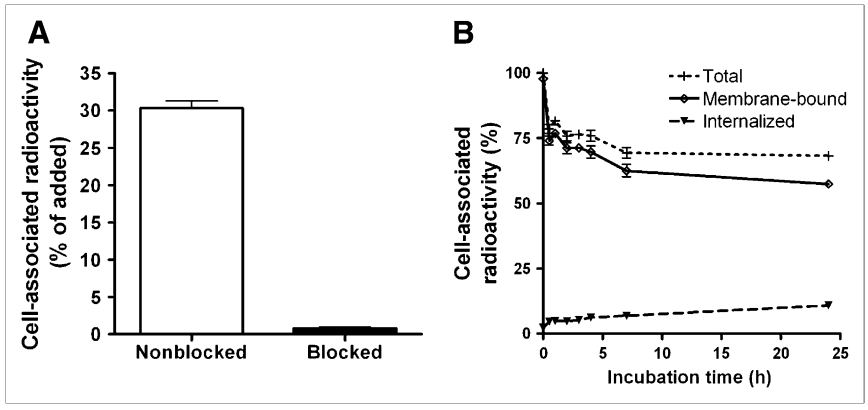

FIGURE 1. (A) In vitro specificity analysis. One group of culture dishes with SKOV-3 cells was pretreated with saturating amounts of nonlabeled His_6-$Z_{HER2:342}$ before incubation with ^{99m}Tc-$Z_{HER2:2395}$-C. Cell-associated radioactivity was calculated as percentage of total added radioactivity. (B) Cell-associated radioactivity as function of time after interrupted incubation of SKOV-3 cells with ^{99m}Tc-$Z_{HER2:2395}$-C. Cell-associated radioactivity at time zero after interrupted incubation was considered to be 100%. Radioactivity that was removed from cells by treatment with 4 M urea solution in 0.2 M glycine buffer (pH 2.0) was considered to be membrane bound, and remainder was considered to be internalized. Data are presented as mean ± SD (n = 3). Error bars may not be visible because they are smaller than the symbols.

TABLE 1. Biodistribution of ^{99m}Tc-H_6-$Z_{HER2:342}$-C in SCID Mice Bearing SKOV-3 Tumors

Tissue	Uptake (%IA/g) at: 1 h	2 h	4 h
Blood	7 ± 2.0	2.7 ± 0.5	1.3 ± 0.4
Heart	3.0 ± 0.5	1.5 ± 0.4	0.7 ± 0.3
Lung	7 ± 1.9	1.8 ± 0.6	1.5 ± 0.3
Liver	19 ± 1.9	17 ± 3.6	19 ± 5
Spleen	2.0 ± 1.0	2.1 ± 0.2	2.0 ± 0.2
Pancreas	0.7 ± 0.2	0.5 ± 0.1	0.40 ± 0.04
Kidney	63 ± 12	89 ± 10	73 ± 9
Stomach	1.4 ± 0.6	1.1 ± 0.1	0.6 ± 0.1
Tumor	6 ± 1.9	8.3 ± 1.6	8.9 ± 3.1
Skin	2.8 ± 0.5	1.3 ± 0.4	1.8 ± 0.5
Muscle	0.4 ± 0.1	0.20 ± 0.03	0.14 ± 0.03
Bone	1.1 ± 0.2	1.3 ± 0.3	0.7 ± 0.2

Data are presented as mean ± SD for 3 animals.

The biodistribution data for ^{99m}Tc-Z_{2395}-C in nude mice bearing LS174T xenografts at 0.5, 1, 2, 4, and 6 h after injection are shown in Tables 2 and 3. Besides the kidneys, the only site with high uptake was the tumor. Tumor uptake was high (7 ± 2 %IA/g) as early as 0.5 h after injection, and it did not change significantly during the experiment. The uptake in all other organs and tissues was low. Generally, tumor-to-organ ratios increased between 0.5 and 6 h because of a decrease in radioactivity in nontarget organs.

The biodistribution data for ^{99m}Tc-Z_{2395}-C in nude mice bearing SKOV-3 xenografts at 4 h after injection are also shown in Tables 2 and 3. The uptake in these xenografts, with high HER2 levels of expression, was also high (15 ± 3 %IA/g), and the tumor-to-blood ratio was 121 ± 24.

The results of the in vivo specificity analysis shown in Figure 3 demonstrated the specificity of uptake. Presaturation of receptors led to a significant decrease in radioactivity uptake in tumors for both LS174T ($P < 0.005$) and SKOV-3 ($P < 0.0005$) xenografts.

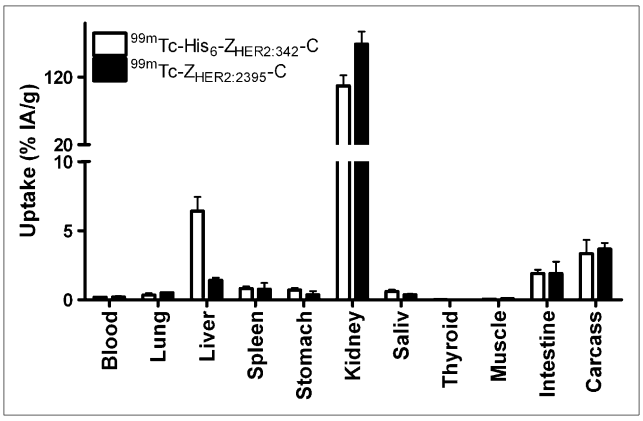

FIGURE 2. Biodistributions of radiolabeled Affibody molecules ^{99m}Tc-H_6-$Z_{HER2:342}$-C, containing His tag, and ^{99m}Tc-$Z_{HER2:2395}$-C, lacking His tag, in NMRI (normal) mice 4 h after injection. Data are expressed as %IA per whole sample for gastrointestinal tract and contents, thyroid, and carcass and as %IA/g for other tissues and are presented as mean ± SD for 4 animals. Saliv = salivary gland.

γ-Camera Imaging

Images acquired 1 and 4 h after the intravenous injection of ^{99m}Tc-Z_{2395}-C into nude mice bearing subcutaneous LS174T or SKOV-3 xenografts confirmed that tumor visualization was feasible as early as 1 h after injection (Figs. 4 and 5). The renal route of elimination of the conjugate led to substantial kidney retention on the images as well. Other organs and tissues were not visualized. The rapid clearance from the blood and nontarget organs allowed for increased contrast at the later time point (4 h after injection). The tumor-to-thigh (contralateral) ratios were 10.0 ± 0.4 (average ± maximum error) for LS174T xenografts and 34 ± 5 for SKOV-3 xenografts 4 h after injection. LS174T xenografts were not visualized in mice preinjected with unlabeled Affibody molecules to saturate HER2. Therefore, the specificity of HER2 imaging of ^{99m}Tc-Z_{2395}-C was confirmed in this experiment. The absence of uptake in HER2-negative A431 xenografts also confirmed the specificity of HER2 targeting.

DISCUSSION

Affibody molecules were proven earlier to be promising tracers for in vivo molecular imaging (*11,30*). The use of ^{99m}Tc as a label would facilitate their rapid implementation in clinical practice because of the favorable properties of this nuclide and its ready availability. The thiophilic nature of technetium(V) enables the site-specific labeling of thiol-containing proteins (*25*), providing a well-defined, homogeneous product. The use of cysteine-based peptide chelators would enable the recombinant production of Affibody molecule–based tracers in a single process with high reproducibility. We previously demonstrated the feasibility of using an N-terminal cysteine to label an anti-HER2 Affibody molecule (*26*). However, elevated uptake in the stomach and salivary glands (3–4 %IA/g 4 h after injection) indicated a certain degree of catabolic instability of the label in vivo. Literature data suggested that using a C-terminal cysteine to label scFv fragments provided catabolically more stable labels (*14,25*). The biodistribution of Affibody molecules and thereby their imaging contrast are influenced by the nature of the chelator–metal complex (*15,19–21,26,29*). Therefore, an in vivo evaluation was necessary for the development of this type of labeling for Affibody molecules.

The introduction of a C-terminal cysteine did not affect the affinity of $Z_{HER2:342}$ for HER2 appreciably and enabled efficient labeling. The initial His tag–containing tracer, ^{99m}Tc-H_6-$Z_{HER2:342}$-C, showed reduced radioactivity uptake in the stomach of tumor-bearing SCID mice (Table 1) relative to literature data on N-terminal cysteine–containing ^{99m}Tc-CGG-$Z_{HER2:342}$. This finding indicated superior stability of the cysteine-containing chelator in the C-terminal position

TABLE 2. Uptake of ^{99m}Tc-$Z_{HER2:2395}$-C in BALB/c *nu/nu* Mice Bearing Xenografts of LS174T or SKOV-3 Tumors

	Uptake* in:				
	LS174T at:				SKOV-3 at:
Tissue	0.5 h	1 h	4 h	6 h	4 h
Blood	2.4 ± 0.2	1.0 ± 0.2	0.08 ± 0.02	0.05 ± 0.02	0.13 ± 0.04
Lung	3.1 ± 0.5	2.0 ± 0.5	0.39 ± 0.07	0.5 ± 0.3	0.45 ± 0.07
Liver	1.7 ± 0.3	2.0 ± 0.4	1.5 ± 0.2	1.7 ± 0.3	1.6 ± 0.1
Spleen	1.3 ± 0.2	1.5 ± 1.3	0.40 ± 0.06	0.38 ± 0.06	0.5 ± 0.2
Stomach	1.9 ± 0.4	1.3 ± 0.4	0.37 ± 0.05	0.36 ± 0.03	0.44 ± 0.08
Kidney	147 ± 20	184 ± 18	191 ± 15	157 ± 18	143 ± 20
Salivary gland	1.1 ± 0.2	0.7 ± 0.2	0.28 ± 0.05	0.28 ± 0.03	0.35 ± 0.07
Thyroid	0.040 ± 0.002	0.026 ± 0.003	0.006 ± 0.001	0.007 ± 0.004	0.005 ± 0.001
Tumor	7.2 ± 2.3	8.7 ± 1.7	6.9 ± 2.5†	6.6 ± 0.8	15 ± 3†
Muscle	0.55 ± 0.08	0.36 ± 0.06	0.2 ± 0.1	0.07 ± 0.01	0.09 ± 0.01
Intestine	2.5 ± 0.4	1.8 ± 0.5	1.5 ± 0.3	2.2 ± 0.5	2.1 ± 0.3
Carcass	153 ± 2.5	9.4 ± 1.1	3.7 ± 0.5	2.8 ± 0.2	3.9 ± 0.4

*Uptake is reported as %IA/g for all tissues except gastrointestinal tract and its contents, thyroid, and carcass, for which uptake is reported as %IA per whole sample.

†Significant difference ($P < 0.05$) between LS174T xenografts (moderate level of HER2 expression) and SKOV-3 xenografts (high level of HER2 expression).

Data are presented as mean ± SD for 4 animals.

rather than the N-terminal position. However, ^{99m}Tc-H_6-$Z_{HER2:342}$-C yielded high liver uptake. To verify that the SCID animal model was not the cause of the high liver uptake, a comparison between SCID and BALB/c *nu/nu* mice was performed. The biodistribution of synthetic ^{111}In-DOTA-$Z_{HER2:342}$ in SCID mice bearing SKOV-3 tumors was compared with the previously described biodistribution of the same conjugate in BALB/c *nu/nu* mice (*17*). The results obtained in the two animal models showed a high level of agreement (Supplemental Table 1). The liver uptake of ^{111}In-DOTA-$Z_{HER2:342}$ in SCID mice was somewhat elevated in comparison with the uptake in BALB/c *nu/nu* mice, but not to such an extent that it could be considered the reason for the high liver uptake of all Affibody molecules, including ^{99m}Tc-H_6-$Z_{HER2:342}$-C, in this animal model. An alternative hypothesis for the high liver uptake was the presence of a His tag in the conjugate. Elevated liver uptake of a His tag–containing conjugate was detected for H_6-$Z_{HER2:342}$-C labeled with ^{111}In when a maleimido derivative of DOTA was used (*29*). Therefore, a variant of HER2-binding Affibody molecule $Z_{HER2:342}$ lacking the His tag but with a C-terminal cysteine, Z_{2395}-C, was evaluated. A comparison of the biodistributions of the His tag–containing conjugate, ^{99m}Tc-H_6-$Z_{HER2:342}$-C, and the corresponding variant lacking the His tag, ^{99m}Tc-Z_{2395}-C, confirmed the negative effect of the His tag on liver uptake (Fig. 2).

^{99m}Tc-Z_{2395}-C showed adequate stability both in vitro and in vivo. Characterization in vitro with HER2-expressing SKOV-3 cells showed that both binding specificity (Fig. 1A) and a high degree of binding capacity were retained after labeling. The cellular retention of ^{99m}Tc-Z_{2395}-C in SKOV-3 cells was good throughout the experiment (24 h), mainly because of strong membrane binding rather than intracellular trapping (Fig. 1B). In vivo, the specificity was

TABLE 3. Tumor-to-Organ Ratios for ^{99m}Tc-$Z_{HER2:2395}$-C in BALB/c *nu/nu* Mice Bearing Xenografts of LS174T or SKOV-3 Tumors

	Tumor-to-organ ratio				
	LS174T at:				SKOV-3 at:
Organ	0.5 h	1 h	4 h	6 h	4 h
Blood	3.1 ± 1.2	9.1 ± 2.2	88 ± 24	129 ± 35	121 ± 24
Lung	2.3 ± 0.6	4.3 ± 0.5	17 ± 6	15 ± 7	34 ± 5
Liver	4.3 ± 1.2	4.4 ± 0.6	4.5 ± 1.4	4.0 ± 0.4	9.3 ± 1.5
Spleen	5.8 ± 1.9	7.8 ± 3.9	17 ± 4	17 ± 1	33 ± 7
Stomach	3.9 ± 1.3	6.7 ± 1.6	19 ± 6	19 ± 3	35 ± 7
Kidney	0.05 ± 0.01	0.05 ± 0.01	0.04 ± 0.01	0.042 ± 0.002	0.11 ± 0.02
Salivary gland	6.4 ± 1.9	12.0 ± 2.6	26 ± 16	24 ± 4	44 ± 9
Muscle	13 ± 5	24 ± 6	60 ± 38	91 ± 22	172 ± 24

Data are presented as mean ± SD for 4 animals.

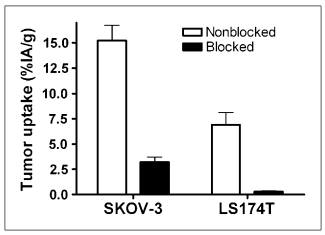

FIGURE 3. Specificity of ^{99m}Tc-$Z_{HER2:2395}$-C tumor uptake in SKOV-3 and LS174T xenografts 4 h after injection. To saturate HER2 in tumors, one group of animals for each tumor model was preinjected with 600 μg of nonlabeled His_6-$Z_{HER2:342}$ 45 min before injection of radiolabeled conjugate (designated as blocked). All animals were injected with 1 μg of labeled Affibody molecule. Data are expressed as %IA/g and are presented as mean ± SD for 4 animals.

confirmed by a blocking experiment, in which presaturation of HER2 in xenografts of two cell lines reduced the tumor accumulation of ^{99m}Tc-Z_{2395}-C (Fig. 3). In LS174T-bearing and SKOV-3–bearing mice a prominent uptake in tumors but very low uptake in normal tissues was shown, resulting in high tumor-to-background ratios. A comparison of the biodistributions of ^{99m}Tc-Z_{2395}-C and ^{99m}Tc-CGG-$Z_{HER2:342}$ (*26*) in SKOV-3–bearing mice 4 h after injection revealed that the radioactivity uptake of ^{99m}Tc-Z_{2395}-C in the stomach and thyroid was strongly reduced—8-fold in the stomach and nearly 40-fold in the thyroid. These numbers indicate that the stability of the ^{99m}Tc-labeled Affibody molecule

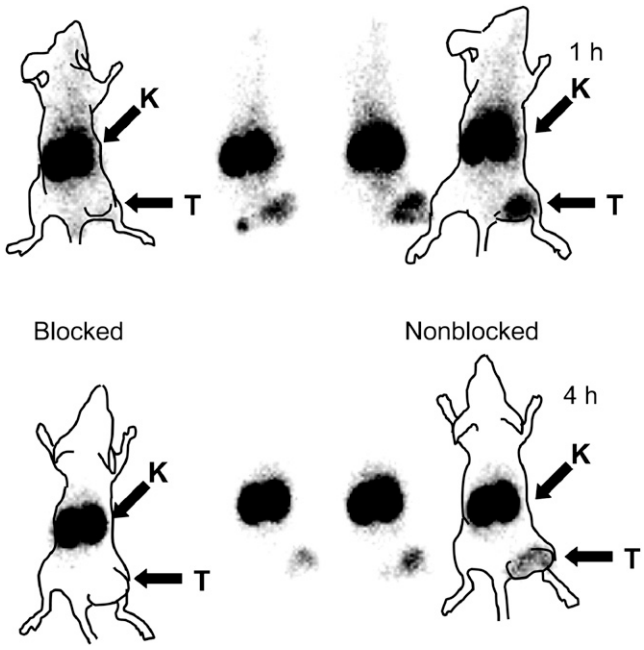

FIGURE 4. Imaging of HER2 expression in LS174T xenografts in BALB/c *nu/nu* mice with ^{99m}Tc-$Z_{HER2:2395}$-C. In blocking experiment, HER2 was saturated by preinjection of 600 μg of nonlabeled Affibody molecule. Planar γ-camera images were acquired 1 and 4 h after administration of ^{99m}Tc-$Z_{HER2:2395}$-C. Tumors (right hind leg) were clearly visualized without blocking but were not seen in blocking experiment, indicating specific HER2 binding to ^{99m}Tc-$Z_{HER2:2395}$-C. Animal contours were derived from digital photographs and superimposed over γ-camera images to facilitate interpretation. K = kidney; T = tumor.

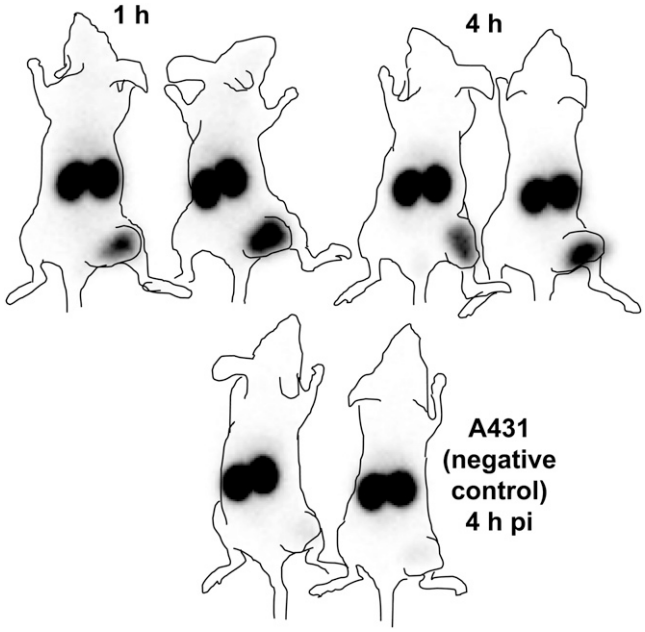

FIGURE 5. Imaging of HER2 expression in SKOV-3 and A431 xenografts in BALB/c *nu/nu* mice with ^{99m}Tc-$Z_{HER2:2395}$-C. A431 tumors were used as negative controls because they are considered to be non–HER2-expressing tumors. Planar γ-camera images were acquired 1 and 4 h after administration of ^{99m}Tc-$Z_{HER2:2395}$-C in mice with SKOV-3 xenografts and 4 h after administration in mice with A431 xenografts. Tumors (right hind leg) were clearly visualized in SKOV-3 xenografts but were not seen in negative controls, indicating specific HER2 binding to ^{99m}Tc-$Z_{HER2:2395}$-C. Animal contours were derived from digital photographs and superimposed over γ-camera images to facilitate interpretation. pi = after injection.

conjugate is improved when the cysteine is placed in a C-terminal position rather than in an N-terminal position. The only organ with high ^{99m}Tc-Z_{2395}-C radioactivity uptake was the kidney. High accumulation in the kidneys is expected for small targeting proteins (<60 kDa) because of reabsorption in the proximal tubules (*31*). Anatomically, the kidneys are well separated from the main metastatic sites for breast cancer, which is the type of cancer for which HER2 imaging primarily will have a clinical application. Therefore, it should be possible to visualize tumors with SPECT/CT without interference from the high accumulation of radioactivity in the kidneys.

^{99m}Tc-Z_{2395}-C showed rapid tumor targeting and rapid clearance from nontarget tissues, thereby enabling high-contrast imaging as early as 1 h after injection (Figs. 4 and 5). The tumor-to-blood ratios increased at the later time points, indicating that optimal contrast enhancement could be achieved once the tracer was allowed to clear from nontarget tissues. The characterization of ^{99m}Tc-Z_{2395}-C revealed the excellent targeting properties of this tracer.

The requirement of high specific radioactivity is not as crucial for HER2-imaging agents as it is for many other tracers because of the very high level of HER2 over-

expression in malignant tumors. For example, an immunohistochemical score of 3+ corresponds to ~2.3 million of these receptors per cell (*32*). Moreover, the presence of shed HER2 can alter the blood kinetics and biodistribution of HER2-targeting agents if the specific radioactivity is too high. The preliminary results of a clinical study on the imaging of HER2 expression in breast cancer with ^{89}Zr-trastuzumab (*33*) showed that for satisfactory imaging, the mass of radiolabeled trastuzumab should be at least 50 mg (~300 nmol) for trastuzumab-naive patients. Preclinical data demonstrated that the levels of uptake of $Z_{HER2:342}$ in SKOV-3 xenografts do not differ significantly for injected masses ranging from 0.1 to 10 μg (14 pmol−1.4 nmol) per mouse (*34*). Therefore, the results of biodistribution experiments with slightly different masses of injected Affibody molecules in mice bearing SKOV-3 xenografts may be directly compared.

The use of another ^{99m}Tc-labeled anti-HER2 tracer, a ^{99m}Tc-hydrazinonicotinamide-trastuzumab Fab fragment, was previously reported (*35*). This tracer yielded a tumor-to-blood ratio of 3.2 ± 0.68 at 24 h after injection in a BT-474 xenograft model with a high level of HER2 expression. In comparison, the smaller ^{99m}Tc-Z_{2395}-C provided contrast nearly 40 times higher as early as 4 h after injection when evaluated in SKOV-3 xenografts, which have a HER2 expression level similar to that in BT-474 xenografts (*36*). The improved contrast is due to higher tumor uptake and to more rapid blood clearance of Affibody molecules than Fab fragments. In comparison with ^{99m}Tc-CGG-$Z_{HER2:342}$, ^{99m}Tc-Z_{2395}-C showed not only improved catabolic stability of the label but also a lower level of hepatobiliary excretion—an advantage for the imaging of extrahepatic abdominal metastases. These data might indicate that hepatobiliary excretion is determined not only by the overall charge and lipophilicity of proteins but also by the regional distribution of amino acids. In comparison with synthetic mercaptoacetyl-containing anti-HER2 Affibody conjugates (*19–21*), Z_{2395}-C showed better affinity, which may have been attributable to the better spatial separation of the chelator and the binding site of the Affibody molecule. This characteristic translated into higher tumor uptake of ^{99m}Tc-Z_{2395}-C and a higher tumor-to-blood ratio. The combination of high affinity, high label stability, and favorable biodistribution properties renders ^{99m}Tc-Z_{2395}-C the best preclinically tested ^{99m}Tc-labeled HER2-imaging tracer to date. The introduction of a C-terminal cysteine to create a technetium chelator also provides more flexibility in the manufacturing of Affibody molecules than can be achieved with mercaptoacetyl derivatives because a species with only native amino acids can be produced in a recombinant fashion.

CONCLUSION

The introduction of a C-terminal cysteine provided a unique site for the labeling of recombinant Affibody molecules with ^{99m}Tc. The tracer ^{99m}Tc-Z_{2395}-C, not containing a His tag, showed efficient targeting of HER2-expressing xenografts and rapid clearance from all normal tissues, except the kidneys. Clear and specific visualization of HER2 expression in a murine xenograft model with ^{99m}Tc-Z_{2395}-C is possible within a few hours after injection, and the tumor-to-blood ratio (121 ± 24 at 4 h after injection in SKOV-3 xenografts) is better for ^{99m}Tc-Z_{2395}-C than for any other ^{99m}Tc-labeled HER2-targeting agent tested. In conclusion, ^{99m}Tc-Z_{2395}-C is a promising SPECT tracer for the detection of HER2 expression in malignant tumors.

ACKNOWLEDGMENTS

This research was financially supported in part by a grant from the Swedish Cancer Society (Cancerfonden) and a research scholarship from the Schuberts Fund.

REFERENCES

1. Hynes NE, Lane HA. ERBB receptors and cancer: the complexity of targeted inhibitors. *Nat Rev Cancer.* 2005;5:341–354.
2. Yarden Y, Sliwkowski MX. Untangling the ErbB signalling network. *Nat Rev Mol Cell Biol.* 2001;2:127–137.
3. Baselga J, Perez EA, Pienkowski T, Bell R. Adjuvant trastuzumab: a milestone in the treatment of HER-2-positive early breast cancer. *Oncologist.* 2006; 11(suppl 1):4–12.
4. Scaltriti M, Baselga J. The epidermal growth factor receptor pathway: a model for targeted therapy. *Clin Cancer Res.* 2006;12:5268–5272.
5. Bast RC Jr, Ravdin P, Hayes DF, et al. 2000 update of recommendations for the use of tumor markers in breast and colorectal cancer: clinical practice guidelines of the American Society of Clinical Oncology. *J Clin Oncol.* 2001;19:1865–1878.
6. Molina R, Barak V, van Dalen A, et al. Tumor markers in breast cancer: European Group on Tumor Markers recommendations. *Tumour Biol.* 2005;26:281–293.
7. Perez EA, Suman VJ, Davidson NE, et al. HER2 testing by local, central, and reference laboratories in specimens from the North Central Cancer Treatment Group N9831 intergroup adjuvant trial. *J Clin Oncol.* 2006;24:3032–3038.
8. Behr TM, Béhé M, Wörmann B. Trastuzumab and breast cancer. *N Engl J Med.* 2001;345:995–996.
9. Perik PJ, Lub-De Hooge MN, Gietema JA, et al. Indium-111-labeled trastuzumab scintigraphy in patients with human epidermal growth factor receptor 2-positive metastatic breast cancer. *J Clin Oncol.* 2006;24:2276–2282.
10. Tolmachev V. Imaging of HER-2 overexpression in tumors for guiding therapy. *Curr Pharm Des.* 2008;14:2999–3019.
11. Tolmachev V, Orlova A, Nilsson FY, Feldwisch J, Wennborg A, Abrahmsén L. Affibody molecules: potential for in vivo imaging of molecular targets for cancer therapy. *Expert Opin Biol Ther.* 2007;7:555–568.
12. Orlova A, Magnusson M, Eriksson T, et al. Tumor imaging using a picomolar affinity HER2 binding Affibody molecule. *Cancer Res.* 2006;66:4339–4348.
13. Mume E, Orlova A, Nilsson F, et al. Evaluation of (4-hydroxyphenyl)ethylmaleimide for site-specific radiobromination of anti-HER2 Affibody. *Bioconjug Chem.* 2005;16:1547–1555.
14. Orlova A, Rosik D, Sandström M, Lundqvist H, Einarsson L, Tolmachev V. Evaluation of [$^{111/114m}$In]CHX-A″-DTPA-$Z_{HER2:342}$, an Affibody ligand conjugate for targeting of HER2-expressing malignant tumors. *Q J Nucl Med Mol Imaging.* 2007;51:314–323.
15. Orlova A, Tran T, Widström C, Engfeldt T, Eriksson Karlström A, Tolmachev V. Pre-clinical evaluation of [^{111}In]-benzyl-DOTA-$Z_{HER2:342}$, a potential agent for imaging of HER2 expression in malignant tumors. *Int J Mol Med.* 2007;20:397–404.
16. Tolmachev V, Nilsson FY, Widström C, et al. ^{111}In-benzyl-DTPA-$Z_{HER2:342}$, an Affibody-based conjugate for in vivo imaging of HER2 expression in malignant tumors. *J Nucl Med.* 2006;47:846–853.
17. Orlova A, Tolmachev V, Pehrson R, et al. Synthetic Affibody molecules: a novel class of affinity ligands for molecular imaging of HER2 expressing malignant tumors. *Cancer Res.* 2007;67:2178–2189.
18. Feldwisch J, Orlova A, Tolmachev V, Baum R. Clinical and pre-clinical application of HER2-specific Affibody molecules for diagnosis of recurrent HER2 positive breast cancer by SPECT or PET/CT [abstract]. *Mol Imaging.* 2006;5(suppl):215.

19. Engfeld T, Orlova A, Tran T, et al. Imaging of HER2-expressing tumours using a synthetic Affibody molecule containing the ^{99m}Tc-chelating mercaptoacetyl-glycyl-glycyl-glycyl (MAG3) sequence. *Eur J Nucl Med Mol Imaging.* 2007;34:722–733.
20. Engfeld T, Tran T, Orlova A, et al. ^{99m}Tc-chelator engineering to improve tumour targeting properties of a HER2-specific Affibody molecule. *Eur J Nucl Med Mol Imaging.* 2007;34:1843–1853.
21. Tran T, Engfeldt T, Orlova A, et al. ^{99m}Tc-maEEE-$Z_{HER2:342}$, an Affibody molecule-based tracer for the detection of HER2 expression in malignant tumors. *Bioconjug Chem.* 2007;18:1956–1964.
22. Orlova A, Nilsson FY, Wikman M, et al. Comparative in vivo evaluation of technetium and iodine labels on an anti-HER2 Affibody for single-photon imaging of HER2 expression in tumors. *J Nucl Med.* 2006;47:512–519.
23. Liberatore M, Neri D, Neri G, et al. Efficient one-step direct labelling of recombinant antibodies with technetium-99m. *Eur J Nucl Med.* 1995;22:1326–1329.
24. George AJ, Jamar F, Tai MS, et al. Radiometal labeling of recombinant proteins by a genetically engineered minimal chelation site: technetium-99m coordination by single-chain Fv antibody fusion proteins through a C-terminal cysteinyl peptide. *Proc Natl Acad Sci USA.* 1995;92:8358–8362.
25. Berndorff D, Borkowski S, Moosmayer D, et al. Imaging of tumor angiogenesis using ^{99m}Tc-labeled human recombinant anti–ED-B fibronectin antibody fragments. *J Nucl Med.* 2006;47:1707–1716.
26. Tran T, Engfeldt T, Orlova A, et al. In vivo evaluation of cysteine-based chelators for attachment of ^{99m}Tc to tumor-targeting Affibody molecules. *Bioconjug Chem.* 2007;18:549–558.
27. Francesconi LC, Zheng Y, Bartis J, Blumenstein M, Costello C, De Rosch MA. Preparation and characterization of [^{99}TcO] apcitide: a technetium labeled peptide. *Inorg Chem.* 2004;43:2867–2875.
28. Davison A, Jones AG, Orvig C, Sohn M. A new class of oxotechnetium(5+) chelate complexes containing a $TcON_2S_2$ core. *Inorg Chem.* 1981;20:1629–1632.
29. Ahlgren S, Orlova A, Rosik D, et al. Evaluation of maleimide derivative of DOTA for site-specific labeling of recombinant Affibody molecules. *Bioconjug Chem.* 2008;19:235–243.
30. Orlova A, Feldwisch J, Abrahmsén L, Tolmachev V. Update: Affibody molecules for molecular imaging and therapy for cancer. *Cancer Biother Radiopharm.* 2007;22:573–584.
31. Behr TM, Goldenberg DM, Becker W. Reducing the renal uptake of radiolabeled antibody fragments and peptides for diagnosis and therapy: present status, future prospects and limitations. *Eur J Nucl Med.* 1998;25:201–212.
32. Ross JS, Fletcher JA, Bloom KJ, et al. Targeted therapy in breast cancer: the HER-2/neu gene and protein. *Mol Cell Proteomics.* 2004;3:379–398.
33. Dijkers E, Lub-de Hooge MN, Kosterink JG, et al. Characterization of ^{89}Zr-trastuzumab for clinical HER2 immunoPET imaging [abstract]. *J Clin Oncol.* 2007;25(suppl):3508.
34. Orlova A, Wållberg H, Tolmachev V. Optimisation of specific radioactivity of Affibody molecule enables in vivo discrimination between high and low HER2 expression [abstract]. *Eur J Nucl Med Mol Imaging.* 2008;35(suppl 2):S187.
35. Tang Y, Scollard D, Chen P, Wang J, Holloway C, Reilly RM. Imaging of HER2/neu expression in BT-474 human breast cancer xenografts in athymic mice using [^{99m}Tc]-HYNIC-trastuzumab (Herceptin) Fab fragments. *Nucl Med Commun.* 2005;26:427–432.
36. Yang D, Kuan CT, Payne J, et al. Recombinant heregulin-Pseudomonas exotoxin fusion proteins: interactions with the heregulin receptors and antitumor activity in vivo. *Clin Cancer Res.* 1998;4:993–1004.